Ore Deposits Research Section
The Pennsylvania State University
University Park, PA 16802

Final Report for October, 1994- September, 1995 on the Project

KINETIC MEASUREMENTS ON THE SILICATES OF THE YUCCA MOUNTAIN POTENTIAL REPOSITORY

to

Los Alamos National Laboratory
August, 1995

H.L. Barnes and R.T. Wilkin

ABSTRACT

This Final Report includes a summary and discussion of results obtained under this project on the solubilities in subcritical aqueous solutions of Mont St. Hilaire analcime, Wikieup analcime, and Castle Creek Na-clinoptilolite. Also included here are the methods and results of hydrothermal flow-through experiments designed to measure the rates of Na-clinoptilolite dissolution and precipitation at 125°C. In this report, high-temperature solubility measurements made in our lab are integrated and discussed along with the low-temperature measurements made at Yale University. The final report prepared by the group at Yale University (Lasaga et al.) includes a synthesis of dissolution rate measurements made between 25° and 125°C on the Na-clinoptilolite.

The temperature dependence of the logarithm of the solubility products of Mont St. Hilaire analcime (log K_{sp1}), Wikieup analcime (log K_{sp2}), and Castle Creek Na-clinoptilolite (log K_{sp3}) in aqueous solutions can be described over the given temperature ranges (in parentheses) by the following equations:

$$\log K_{sp1} = 326.07 - 24{,}199.4/T - 106.73 \log T \quad (25°\text{-}300°C)$$

$$\log K_{sp2} = 94.59 - 9{,}928.2/T - 31.10 \log T \quad (90°\text{-}225°C)$$

$$\log K_{sp3} = 467.97 - 35{,}814.0/T - 152.59 \log T \quad (25°\text{-}265°C)$$

where T is in Kelvin. These solubility products are based on reactions between the respective zeolites with liquid water to produce aqueous Na^+, $Al(OH)_4^-$, and $Si(OH)_4$. The equations above give log K_{sp}'s that are generally within ±0.3 log units of the measured values presented in this report. Results of the solubility experiments discussed here were presented at the V.M. Goldschmidt Conference held at The Pennsylvania State University on May 25, 1995 in a paper titled *Solubilities of the Zeolites Analcime and Na-clinoptilolite in Hydrothermal Solutions,* by R.T. Wilkin and H.L. Barnes.

INTRODUCTION

Zeolite minerals are widespread authigenic alumino-silicates that form during water-rock interactions at temperatures below roughly 250°C and 2 kb. Silicic and basaltic glasses are common substrates that promote the nucleation and growth of silica-rich (i.e., clinoptilolite, mordenite, and erionite) and silica-poor (i.e., phillipsite and natrolite) zeolites, respectively (Boles, 1985). The predominate geologic settings in which authigenic zeolite formation occurs are (Hay, 1978): *i*) deep-sea pelagic sediments (Kastner and Stonecipher, 1978; Gingele and Schulz, 1993); *ii*) near-surface

environments where alkaline meteoric waters interact with volcanic rocks (Surdam and Sheppard, 1978); *iii*) active geothermal regions (Kristmannsdottir and Tomasson, 1978); and *iv*) in low-grade burial metamorphic environments (Iijima and Utada, 1966). An abundant supply and unique ion-exchange capacities of many natural zeolites and analogous synthetic materials have led to their prevalent use in the agricultural, environmental, and petroleum industries (Mumpton, 1978).

Perhaps the most abundant zeolites in nature are analcime and clinoptilolite which are common to all of the above zeolite-forming environments. Their prevalence in the rhyolitic tuffs at Yucca Mountain, Nevada, a potential repository for high-level radioactive wastes, has stimulated research efforts on their physicochemical properties (e.g., Bish, 1984; Bowers and Burns, 1990; Pabalan, 1994). In particular, clinoptilolite has received much attention because of its cation exchange properties and potential to immobilize certain radionuclide cations. However, the prediction of diagenetic pathways and transformations involving the zeolites and other clay minerals is hindered in part by a lack of appropriate thermodynamic data that accounts for compositional variations. Because zeolite assemblages in tuffaceous sediments apparently represent non-equilibrium assemblages, kinetic factors that control rates of dissolution and precipitation are of paramount importance in modeling the formation and evolution of zeolite-bearing mineral assemblages resulting from continued water-rock interactions.

Thermodynamic data for the zeolites analcime, clinoptilolite, heulandite, mesolite, mordenite, natrolite, phillipsite, scolecite, and stilbite obtained from calorimetric measurements are reported in Johnson et al. (1982, 1983, 1985, 1992), Hemingway and Robie (1984), and Howell et al. (1990); however, the determination of

zeolite solubilities in aqueous solutions has heretofore been avoided because of the expected formation of secondary phases and slow reaction rates at the temperatures of most interest, below 200°C (e.g., Johnson et al., 1982). Here we report the aqueous solubilties of a high-Si sedimentary analcime (Wikieup, AZ) from 25°-225°C, a low-Si hydrothermal analcime (Mont St. Hilaire, Quebec) from 25°-300°, and Na-clinoptilolite (Castle Creek, ID) from 25° to 265°C all at vapor-saturated pressures. The results of these solubility experiments provide a new set of standard free energies of formation for these minerals as a function of temperature as well as a basis for relating measurements of reaction rates of these respective phases to departures from equilibrium. Dissolution rate measurements for Na-clinoptilolite are reported and discussed in a companion paper (MacInnes et al., in prep).

EXPERIMENTAL DESIGN AND METHODS

Materials Selection and Pretreatment

The requirements of starting materials for use in solubility and kinetic experimental studies are: *i*) materials must be free of impurity phases; *ii*) mineral compositions must be uniform and well characterized; and *iii*) individual grains must be coarser than about 1 μm and free of excess surface energy and the strain invariably produced during crushing and sampling handling. Methods used to prepare starting materials meeting the above criteria are discussed below. Analcime from Mont St. Hilaire (Quebec, Canada), a hydrothermal deposit, and Wikieup (Arizona, U.S.A), a sedimentary deposit, were used in solubility experiments. These analcimes formed under different physicochemical conditions and consequently represent near-end-member

analcime composition types. The clinoptilolite from Castle Creek (Idaho, U.S.A.) was donated by Dr. F. Aplin (Pennsylvania State University). Because of their high zeolite content (~95%), bulk material from these deposits required a minimum of physical separations.

Mont St. Hilaire analcime was purchased from Ward's Scientific. Approximately 200 grams of analcime grains free of visible impurities were hand-picked, carefully crushed in an agate mortar, and sieved to recover the 75 μm to 125 μm size fraction. The analcime powder was then repeatedly washed with doubly distilled and deionized water (DDD) in an ultrasonic cleaner to remove adhered ultra-fine particles. After ultrasonic cleaning, the powder was annealed at 125°C in a stainless steal autoclave for 2 weeks. The final cleaned powder was characterized by X-ray diffraction (XRD; Rigaku Geigerflex) to determine mineral content, and scanning electron microscopy (SEM; ISI SX-40A) to determine particle morphology and uniformity of particle size. Major element abundances were determined by inductively-coupled plasma spectroscopy (ICPS; Leeman Labs PS3000). Analytical accuracy and precision of the ICP measurements are within 3% at the 2σ confidence level based on analytical reproducibility of NIST-traceable standards. Zeolite water content was determined by the percent weight loss of samples placed in porcelain crucibles heated to 750°C overnight followed by an additional 2 hours at 900°C. Duplicate and triplicate trials agreed to ±2%. Analytical data and the calculated chemical formula of the Mont St. Hilaire analcime are shown in Table 1 and indicate a nearly stoichiometric composition with Si/Al=2.0. An XRD pattern and SEM photomicrographs tracking the results of the solid pre-treatment steps are included in Appendix A.

Table 1. Chemical analyses (upperset) and structural stoichiometry (lowerset) of analcime and clinoptilolite samples used in this study.

	Mont St. Hilaire Analcime	Wikieup Analcime	Castle Creek Clinoptilolite	Castle Creek Na-clinoptilolite
SiO_2	55.20	58.70	65.50	64.90
TiO_2	< 0.02	0.06	0.08	0.08
Al_2O_3	23.20	19.50	12.40	12.20
Fe_2O_3	<0.02	0.78	0.48	0.90
MgO	<0.02	0.22	1.07	0.07
CaO	0.10	0.17	0.72	0.06
MnO	0.01	0.01	<0.01	0.01
Na_2O	14.10	12.10	3.57	7.24
K_2O	0.10	0.30	2.34	0.25
LOI	7.21	8.53	12.90	13.80
Total	99.92	100.37	99.06	99.51
Si	2.00	2.14	4.91	4.90
Al	1.00	0.84	1.08	1.09
Mg	0.00	0.01	0.12	0.00
Ca	0.00	0.01	0.06	0.00
Na	0.99	0.86	0.52	1.06
K	0.00	0.01	0.21	0.02

Notes: LOI = loss on ignition. Number of cations normalized to 6 oxygens for analcime and 12 oxygens for clinoptilolite, respectively.

About 10 g of analcime from Wikieup was donated by Dr. D. Bish (Los Alamos National Laboratory). We characterized this material using the above techniques (Table 1). The composition of this sedimentary analcime is distinctly non-stoichiometric with an Si/Al ratio of 2.54.

Material from the Castle Creek deposit is exceptionally high in its clinoptilolite content (Mondale et al., 1988) and contains only about 5% of a smectitic clay as the primary impurity. The bulk material was crushed in an agate mortar and sieved through a 100 μm screen. To remove the smectite, about 50 grams of the sieved material was placed in a 1 L graduated cylinder along with a magnetic stirring bar and DDD water. The contents of the cylinder were stirred for *ca.* 10 minutes, then the suspension was allowed to settle for *ca.* 5 minutes before decanting the overlying fluid. The process was repeated several times. The supernatant fluid was enriched in a mixed-layer clay (~90% smectite, 10% illite) and very fine-grained clinoptilolite (<3 μm).

We took advantage of the cation exchange properties of clinoptilolite to prepare Na-clinoptilolite in order to simplify the interpretation of the solubility results and to gain reliable thermodynamic data on the Na-endmember composition. About 150 grams of purified clinoptilolite was treated with 500 mL of 5 *m* NaCl at 120°C for approximately 1000 hours. The NaCl solution was refreshed 6 times during the Na-exchange experiment. The final material was repeatedly washed with DDD water and dried under high humidity at 60°C. The major element compositions and structural formulas of the Na-clinoptilolite and original, unexchanged clinoptilolite are given in Table 1. There was no significant change in the Si/Al ratio during the exchange indicating that formation of unwanted phases did not occur. The divalent cations,

calcium and magnesium, were largely removed during the exchange, although a minor amount of potassium remained within the zeolite (0.25 wt.% K_2O). An XRD pattern and SEM photomicrographs of the Na-clinoptilolite are shown in Appendix A.

Solubility Experiments

The hydrothermal solubilities of Na-clinoptilolite and Mont St. Hilaire analcime were measured using Ti-17 alloy or gold-plated, stainless steel autoclaves (nominal volume 1100 mL) placed in a rocking, dual-wound furnace (Barnes, 1971; Bourcier and Barnes, 1987). Temperature was monitored and controlled using two chromel-alumel thermocouples (Thermoelectrics Company) inserted into the top and bottom of the autoclave. The thermocouples were calibrated with a Pt-resistance thermometer read with a Mueller bridge, DC power supply, and galvanometer. The Mueller bridge gives a measurement of resistance to $\pm 0.0005\Omega$ corresponding to a sensitivity of about $\pm 0.005°C$. The 2σ uncertainty in the temperatures reported here are within $\pm 1.5°C$. Experiments were conducted at pressures along the liquid-vapor curve of the aqueous solutions.

At the beginning of an experiment, 30-50 grams of zeolite powder was placed in the autoclave along with about 400 mL of nitrogen-gas-purged, doubly distilled, deionized water. The autoclave was then flushed with nitrogen gas, sealed, and placed in the furnace. Next, rocking was begun to ensure mixing between the solution and solids and the system heated to the desired temperature. The system was maintained at a constant temperature generally for a minimum of several days at each condition where the solubility was to be determined. Solubility measurements were made by sampling

solutions when approached from undersaturation and also from supersaturation, and by taking multiple samples at a single temperature over increasing intervals of time. Solution sampling was carried out at temperature and pressure using a double-valve configuration (e.g., Gammons and Barnes, 1989). Approximately 8 mL of solution were collected into a plastic syringe and filtered through an 0.2 μm cellulose acetate syringe filter (Nalgene). The room temperature pH was measured on a 3 mL aliquot with a semi-micro combination electrode (Corning) calibrated with NIST-traceable standard buffers. The remaining solution was diluted with doubly distilled and deionized water (DDD) and Ultrex HNO_3. All solutions were analyzed for total Si, Al, and Na by ICP spectroscopy. With these methods, analytical precision and accuracy was better than ±5%. The measured concentrations of Si, Al, and Na in replicate samples also generally agreed to ±5%.

At the end of a run, the autoclave was opened and the contents washed with DDD water and dried. In most cases, powder X-ray diffraction and SEM analyses did indicate the presence of secondary phases that formed during the solubility experiments. However, we could not determine the solubility product of Na-clinoptilolite at temperatures above 265°C because the high concentrations of aqueous silica generated by the dissolving clinoptilolite at these elevated temperatures led to the precipitation of quartz along the vapor-liquid interface within the autoclave.

The solubility of Wikieup analcime was measured at 90°, 125°, 175°, and 225°C using sealed silica tubes placed within a rocking furnace, methods different for this material because of the relatively small amount available. In a silica tube sealed at one end, approximately 500 mg of the analcime was placed plus ~10 mL of N_2-purged DDD

water. The tube was then flushed with Ar gas, sealed, and placed in the furnace which was rocked to again ensure mixing between solid and solution in the silica tubes. After several days, a tube was pulled from the furnace, quenched in ice water, and cracked open. Then the solution was filtered and measurements made of pH, and Si, Al, and Na concentrations.

Evaluation of Experimental Data

Calculation of thermodynamically valid solubility products (K_{sp}) from the measured concentrations of ΣAl, ΣNa, and ΣSi coexisting with the zeolites requires: *i*) knowing the dominant, stoichiometrically balanced dissolution reaction; *ii*) a method of partitioning total analytical concentrations into the appropriate aqueous speciation; and *iii*) an ion activity model to calculate activity coefficients for all aqueous species. The solutions were speciated at temperature using the computer program SOLMINEQ (Kharaka et al., 1988). This program calculates individual ion activity coefficients using the 'B-dot' method of the extended Debye-Hückle equation (Helgeson, 1969). Because buffered solutions were not utilized in these experiments to control pH, solution ionic strengths were solely derived from the products of dissolution and consequently, remained low resulting in small activity corrections. For the neutral species, H_4SiO_4, activity coefficients were derived from data on the solubility of amorphous silica as a function of temperature and salinity (Chen and Marshall, 1982; Kharaka et al., 1988), but these coefficients never significantly departed from unity. In addition to the thermodynamic data included with SOLMINEQ, we have used the recent thermodynamic

data on aqueous aluminum speciation (e.g., Castet et al., 1993; Bourcier et al., 1993; Wesolowski and Palmer, 1994).

At the measured pH of all solutions collected (6.8-9.3 at 25°C), aqueous Al and Si species were dominantly $Al(OH)_4^-$ and $Si(OH)_4$, respectively. Thus, the solubility product for Mont St. Hilaire analcime (an) and Na-clinoptilolite (cp), for instance, can be determined from the following stoichiometric dissolution reactions:

$$Na_{0.99}K_{0.01}AlSi_2O_6 \cdot 1H_2O(an) + 5.0H_2O(l) \Leftrightarrow$$

$$0.99Na^+ + 0.01K^+ + Al(OH)_4^- + 2Si(OH)_{4(aq)}, \qquad (1)$$

and,

$$Na_{1.06}K_{0.03}Al_{1.1}Si_{4.9}O_{12} \cdot 3.5H_2O(cp) + 8.5\ H_2O(l) \Leftrightarrow$$

$$1.06Na^+ + 0.03K^+ + 1.1Al(OH)_4^- + 4.9Si(OH)_{4(aq)}. \qquad (2)$$

The contribution of potassium and other alkali elements have been neglected in the calculation of the solubility product. The molar [Na/Na+K], [Na/Na+Ca], and [Na/Na+Mg] values of the Na-clinoptilolite used in this study, for example, are 0.98, 0.99, and 0.99, respectively; thus, errors accrued by omitting the contribution of these elements to the solubility product are negligible compared to other experimental and analytical uncertainties.

Zeolite minerals exhibit a wide variations in water content. The absolute quantity of water in a particular zeolite can vary depending on temperature, humidity, and exchangeable cation composition (Boles, 1972). An advantage of aqueous solubility measurements on zeolites is that a constant state of maximum hydration can be maintained. Thus, in all calculations analcime and clinoptilolite were assumed to be in a fully hydrated state.

RESULTS AND DISCUSSION

The results of all zeolite solubility vs. temperature measurements made at Yale University and the Pennsylvania State University, respectively, are given in Fig. 1. All solubilities were determined at pressures equivalent to the saturated vapor pressure at each temperature. Where individual data points are closely spaced on Fig. 1, supplementary arrows are shown to indicate the direction of approach to equilibrium prior to sampling, i.e., from either undersaturation or supersaturation. At temperatures below 100°C solubilities were generally only determined from undersaturated conditions; whereas, at temperatures >100°C solubilities were generally approached from both directions because of substantially increased rates of dissolution and precipitation at elevated temperatures.

In Appendix B all experimental data are tabulated including: run temperature, run duration, concentrations of ΣSi, ΣAl, and ΣNa, pH, direction of sampling approach, and calculated log K_{sp} for each zeolite. The temperature-dependent solubility products and their standard errors given in Table 2 were calculated by averaging the set of K_{sp}'s determined at each condition. These values are a direct measurement of the free energy change of the dissolution reaction (ΔG_R°) and are used to derive thermodynamic quantities as discussed below.

For any equilibrium reaction at a constant pressure and a given temperature, the relationship between the reaction free energy, enthalpy, and entropy is given by:

$$\Delta G_R^\circ = \Delta H_R^\circ - T\Delta S_R^\circ. \qquad (3)$$

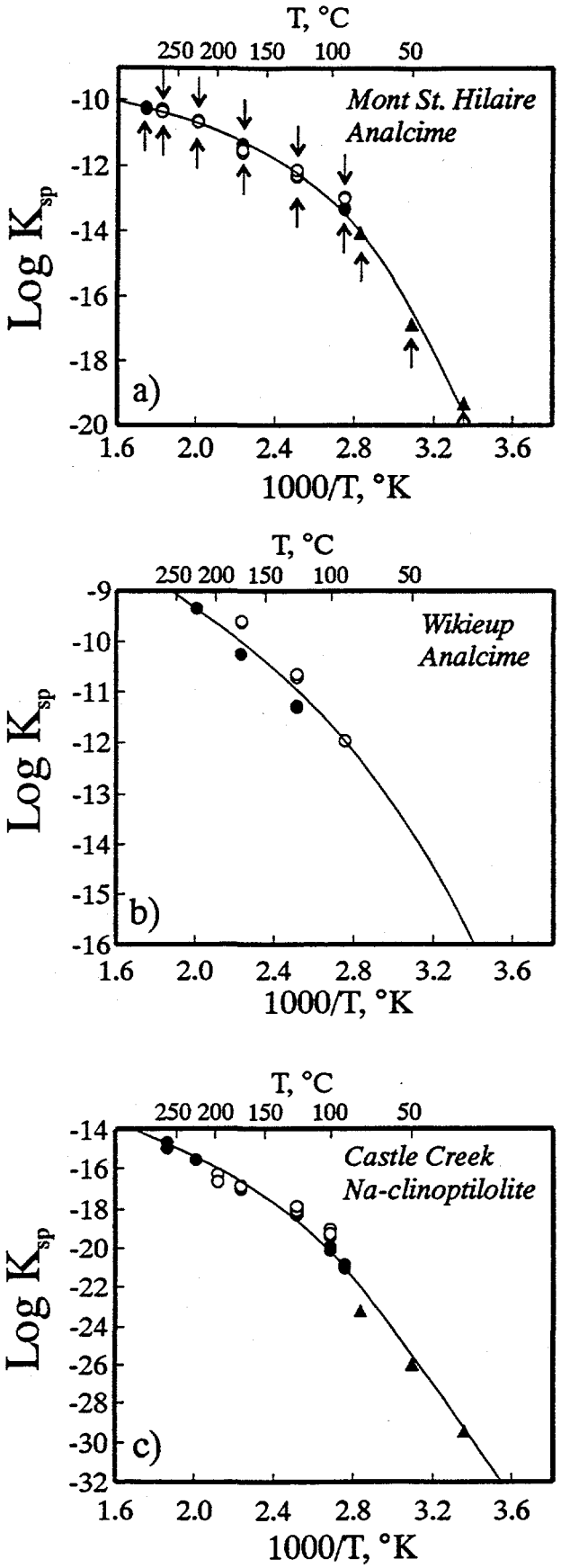

Fig. 1. Log K_{sp} vs. 1000/T plots for a) Mont St. Hilaire analcime; b) Wikieup analcime; and c) Castle Creek Na-clinoptilolite. Filled circles indicate sampling approached from undersaturation; open circles indicate sampling approached from supersaturation. Filled trianglesare measurements made at Yale University (approached from undersaturation).

Table 2. Log K_{sp} values determined in this study (1σ)

Temperature (°C)	Mont St. Hilaire Analcime	Wikieup Analcime	Castle Creek Na-clinoptilolite
25	-19.34		-29.46
50	-16.89		-26.02
80	-14.02		-23.23
90	-13.08(±0.20)	-12.04 (±0.50)	-20.96 (±0.50)
100	---	---	-19.26 (±0.48)
125	-12.21 (±0.17)	-10.98 (±0.36)	-18.07 (±0.49)
175	-11.50 (±0.09)	-9.92 (±0.37)	-16.88 (±0.09)
200	---	---	-16.47 (±0.26)
225	-10.62 (±0.04)	-9.35 (± 0.35)	-15.44 (±0.24)
265	---	---	-14.81 (±0.17)
275	-10.28 (±0.04)	---	---
300	-10.23 (±0.02)	---	---

In terms of equilibrium constants, for instance solubility products, K_{sp}, equation (3) becomes:

$$-2.303\ RT \log K_{sp} = \Delta H_R^\circ - T\Delta S_R^\circ \qquad (4)$$

or

$$\log K_{sp} = -\frac{\Delta H_R^\circ}{2.303RT} + \frac{\Delta S_R^\circ}{2.303R}. \qquad (5)$$

Equation (5) indicates that if log K_{sp} values are measured over a range of temperature then plots of log K_{sp} against 1/T will be linear and the values of ΔH_R° and ΔS_R° derivable from the slope and intercept, respectively, providing that that reaction enthalpies and entropies are independent of temperature over the experimental temperature range. For many equilibrium systems, and specifically for the zeolite solubilities reported here, plots of log K_{sp} against 1/T show significant curvature (Fig. 1) indicating the unreliable assumption of temperature-independent ΔH_R° and ΔS_R°. Non-linearity of solubility products with 1/T is common in reactions between solids and aqueous solutions because of the substantial decrease of the dielectric constant of water that occurs as temperatures increases and the consequent effect of the lowered dielectric constant on the thermodynamic properties of aqueous species.

Examples of the time-dependence of the isothermal solubilities approached from undersaturated and supersaturated conditions are shown in Fig. 2 for the Mont St. Hilaire analcime at 175°C, and the Na-clinoptilolite at 125°C. These data clearly show that the measured concentrations of ΣAl, ΣNa, and ΣSi represent the steady state solubility of the respective zeolites at each temperature. However, the measured concentrations of ΣAl, ΣNa, and ΣSi from the Na-clinoptilolite solubility experiments indicate that the solutions

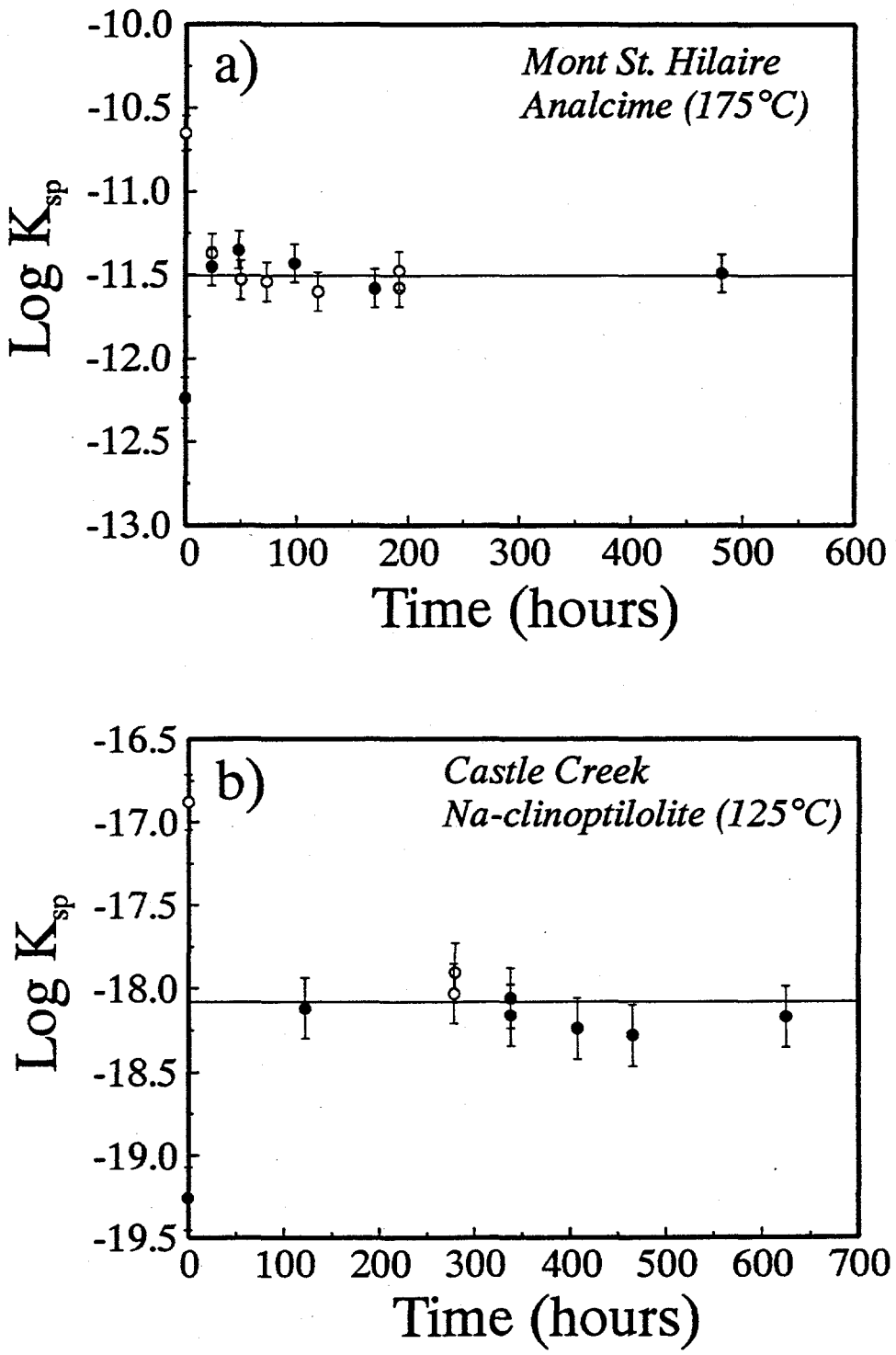

Fig. 2. Isothermal, time-dependent solubility products of a) Mont St. Hilaire analcime (eqn. 1) and b) Castle Creek Na-clinoptilolite (eqn. 2).

are supersaturated with respect to a number of silica, alumino-silicate and sodium-aluminum-silicate phases. For example, the saturation indices (SI) of solutions in apparent equilibrium with Na-clinoptilolite with respect to analcime can be computed as follows:

$$SI = a_{Na^+}^{0.99} a_{Al(OH)_4^-} a_{Si(OH)_4}^2 / K_{an} \quad (6)$$

where a is the activity of the respective aqueous species and K_{an} is the solubility product of analcime (see equation (1)). Saturation indices calculated from equation (6) range from 3 to 25 and tend to increase with increasing temperature. Furthermore, the experimental solutions were always supersaturated with respect to both quartz and cristobalite in the Na-clinoptilolite runs. Yet SEM examination and XRD analyses of the clinoptilolite after experimental runs indicate that these phases did not precipitate during the solubility experiments. This is apparently because the concentrations of solutes required for homogeneous nucleation of these other, more stable phases was not exceeded. As temperature increases, the frequency of homogeneous nucleation is expected to increase (Nielsen, 1964). This assumption was confirmed in an experiment where a mixture of Na-clinoptilolite and water was heated to 300°C. In this experiment, because of the high concentrations of silica generated by the dissolving clinoptilolite, quartz nucleation and growth occurred along the liquid-vapor interface in the sealed autoclave; thus, the maximum temperature at which the solubility of Na-clinoptilolite could be determined without the formation of secondary phases was about 265°C.

Derivation of Thermodynamic Constants

The log K_{sp}'s for the zeolites listed in Table 2 may be used to calculate their standard free energies of formation as a function of temperature. For the Mont St. Hilaire analcime:

$$\Delta G_R^\circ = -2.303RT \log K_{sp} \quad (7)$$

thus, following reaction (1):

$$\Delta G_{f,an}^\circ = 0.99\Delta G_{f,Na+}^\circ + \Delta G_{f,Al(OH)4-}^\circ + 2\Delta G_{f,Si(OH)4}^\circ - \Delta G_R^\circ - 5\Delta G_{f,H2O}^\circ. \quad (8)$$

Equation (8) was evaluated using the ΔG_f° of $Na^+_{(aq)}$ and $H_2O_{(l)}$ tabulated in Cobble et al. (1982). The standard free energy of formation of the aqueous species $Al(OH)_4^-$ as a function of temperature was calculated using the recommended thermodynamic properties of boehmite (Bourcier et al., 1993) and the dissociation constants of boehmite in alkaline solutions given by Castet et al. (1993), respectively. Similarly, the standard free energy of formation of the molecular species $Si(OH)_4$ was calculated using the temperature-dependent solubility of quartz given by Rimstidt and Barnes (1980) and the standard free energies of liquid water given by Cobble et al. (1982). These thermodynamic constants, along with the estimated zeolite standard free energies of formation, are tabulated in Appendix C. The standard state conventions adopted here are the pure liquid and solid at temperature and corresponding vapor-saturated pressure. Assessment of the error in calculated free energies of formation of the zeolites is made by summing the errors in each of the ΔG values in equation (8). The uncertainty in the calculation of free energies using this method is dominated by the reaction free energy measurement (eq. (7)). An uncertainty of 0.50 log units in the measured K_{sp} values

corresponds to about ±3 kJ/mol at 298°K. A total of 5 kJ/mol is considered to be a minimum estimate of error on the calculated standard free energies of formation given in Appendix C.

The standard free energies of formation of the Wikieup and Mont St. Hilaire analcimes determined in this study are shown in Fig. 3 and are directly compared to the previously determined calorimetric values of Johnson et al. (1982). The extrapolated linear trends of ΔG_f° with temperature of the three different analcimes are approximately parallel, indicating that each have similar molar heat capacity functions. The free energies estimated from the solubility measurements at the lowest temperatures fall slightly below the trend extrapolated from high temperatures because of extremely slow rates of dissolution at low temperatures. The Gibbs free energy values of the high-Si analcime from Wikieup are less negative by about 50 kJ/mol compared to the Mont St. Hilaire analcime. The Gibbs free energy values of the low-Si analcime from Mont St. Hilaire are slightly more negative than those determined by Johnson et al (1982) for an analcime with Si/Al=2.13 from Skookumchuck Dam, Washington. The ΔG_f° at 25°C of the respective analcimes are plotted against their corresponding Si/Al ratios in Fig. 4. This plot shows the relationship:

$$\Delta G^\circ_{f,anss} = \Delta G^\circ_{f,an} + 98.8(Si/Al - 2) \qquad (9)$$

where $\Delta G^\circ_{f,anss}$ is the standard free energy of an analcime with variable Si/Al between 2.0 and 2.6, and $\Delta G^\circ_{f,an}$ is the free energy of formation of stoichiometric Mont St. Hilaire analcime (Si/Al=2.0). This thermodynamic model of the analcime solid solution

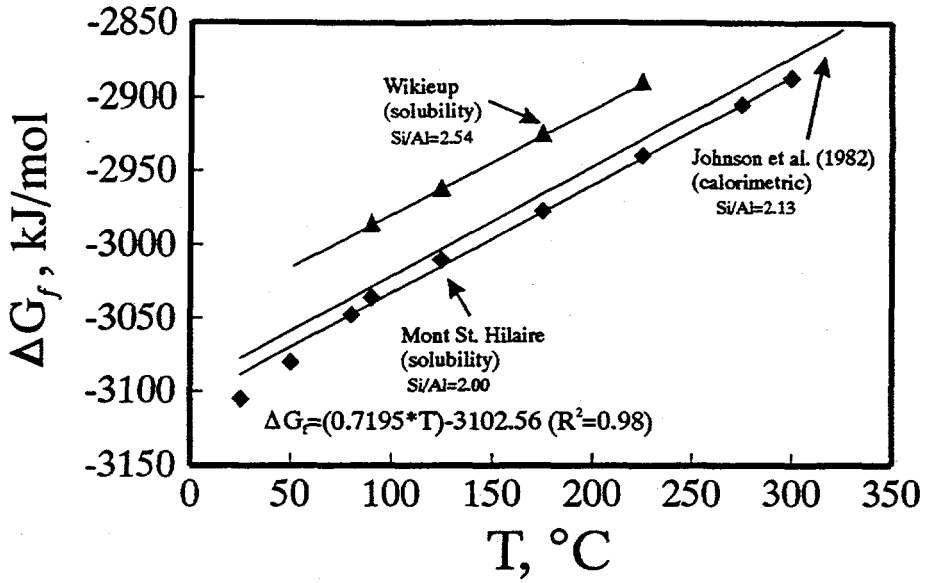

Fig. 3. Standard free energy of formation for analcime with temperature. Linear regression of data is given for the Mont Hilaire analcime.

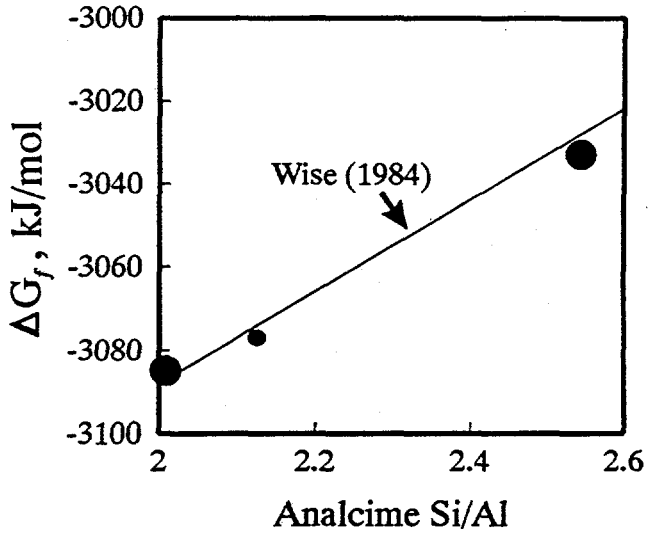

Fig. 4. Standard free energy of formation of analcime at 25°C as a function of Si/Al. Also plotted is the ideal solid solution model of Wise (1984).

is in reasonable agreement with the ideal mixing model presented by Wise (1984)(Fig. 4).

The only available values for the Gibbs free energy of formation for clinoptilolite have been estimated by Bowers and Burns (1990) using the measured heat-capacity and entropy data in Hemingway and Robie (1984). Bowers and Burns (1990) give a ΔG_f° at 25°C of -6316 ±38 kJ/mol for clinoptilolite with the composition:

$$Na_{0.09}K_{0.16}Ca_{0.25}Mg_{0.21}Al_{1.11}Si_{4.83}O_{12}\cdot 3.67H_2O.$$

Our estimated Gibbs free energies of formation for Na-clinoptilolite are shown in Fig. 5. Our measured value of ΔG_f° at 25°C is -6263 ± 15 kJ/mol. This value may be slightly low because of the slow approach to equilibrium at low temperatures; thus a probably better estimate is made by regressing the data from 80°-265°C to 25° which gives -6260 ±15 kJ/mol. This value is preferred because it is weighted by reversible solubility measurements. A direct comparison between the value presented here for Na-clinoptilolite and the value estimated by Bowers and Burns (1990) is complicated by differences in the exchangeable cation composition (see Table 1), Si/Al ratio, and water content between the two clinoptilolites. Clearly there is a need to further explore the thermodynamic constants within the clinoptilolite solid solution.

Geologic Implications

In order to assess the stability limits of clinoptilolite in aqueous solutions and to constrain possible diagenetic transformations of clinoptilolite due to changing water chemistry, Bowers and Burns (1990) constructed activity diagrams using measured and

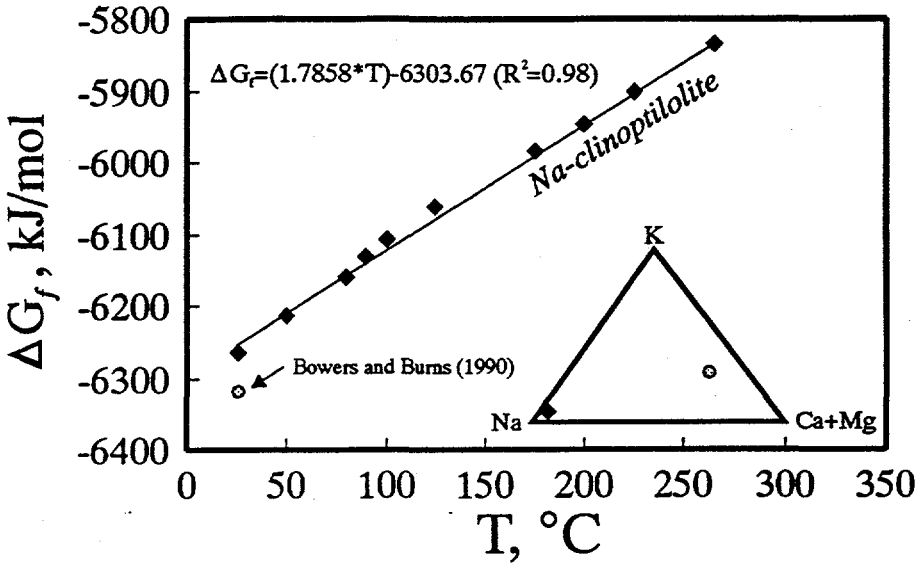

Fig. 5. Standard free energy of formation as a function of temperature of Na-clinoptilolite with linear regression. Also plotted is the estimated free energy of formation at 25°C of a solid solution clinoptilolite (Bowers and Burns, 1990); the composition is indicated in the ternary diagram (half-tone circle).

estimated thermodynamic data for silicate minerals, aqueous species and water in the multi-component system Na-K-Ca-Mg-Fe-Al-Si plus H_2O. An important conclusion of their study was that clinoptilolite formation and persistence is favored only when aqueous silica activities exceed those allowed for by quartz solubility. The common association in natural assemblages of clinoptilolite with opal-CT is then consistent with the calculated wide stability field of clinoptilolite in solutions saturated with cristobalite or amorphous silica. The solubility data presented here also show that high concentrations of silica result from clinoptilolite-water reactions. Measured concentrations of silica generated by dissolving clinoptilolite in the solubility experiments were typically between cristobalite- and amorphous silica-saturation. The high silica concentrations were most apparent in experiments at temperatures greater than 265°C where silica concentrations promoted quartz nucleation along the liquid-vapor interface of the sealed autoclave. Therefore, the persistence of clinoptilolite apparently requires the suppression of quartz nucleation and growth.

The spatial distribution of clinoptilolite and analcime in sedimentary and volcanic-hosted occurrences implies that analcime is produced by replacement reactions of early-formed zeolites including clinoptilolite (e.g., Hay, 1966; Sheppard and Gude, 1969; Bish and Aronson, 1993). Based on microanalytic techniques, Sheppard and Gude (1969) suggested that high-Si analcimes form by replacement reactions of high-Si precursor zeolites such as clinoptilolite and erionite; whereas, low-Si analcimes form by replacement of low-Si zeolite precursors such as phillipsite. In an experimental study, Boles (1971) also found a strong correlation between Si/Al ratios of precursor clinoptilolites and Si/Al ratios in synthetic analcimes. Although the replacement

mechanism is not understood, the apparent conservation of Si and Al suggests that the replacement does not proceed by a dissolution and precipitation process, but rather by structural rearrangement of clinoptilolite.

As part of a modeling study addressing water-rock interactions at Yucca Mountain, Kerrisk (1983) concluded that the clinoptilolite-to-analcime transition is controlled by the activity of silica, where analcime formation is favored at silica activities equivalent to quartz saturation. Assuming conservation of Al and Si, a reaction between Castle Creek Na-clinoptilolite and Mont St. Hilaire analcime can be written as follows:

$$0.91Na_{1.1}Al_{1.1}Si_{4.9}O_{12}\cdot 3.5H_2O(cp) + 2.74H_2O(l) \Rightarrow$$

$$NaAlSi_2O_6\cdot 1H_2O(an) + 2.46Si(OH)_4(aq) \qquad (10)$$

The equilibrium constant for reaction (10) is:

$$K_{10} = \frac{a_{an}\, a^{2.46}_{Si(OH)_4}}{a_{cp}\, a^{2.74}_{H_2O}} \qquad (11)$$

where a is the activity of the zeolites, liquid water, and aqueous silica species, respectively. The temperature-dependent equilibrium constant defined in equation (11) has been calculated using the best-fit free energy of formation data for Mont St. Hilaire analcime and Na-clinoptilolite shown in Figs. 3 and 5, respectively, and the free energies of formation of liquid water listed in Appendix C. If the activities of the solids and water are taken as unity, then equation (11) can be solved to give an activity of $Si(OH)_4$ at which clinoptilolite is in equilibrium with analcime. This critical activity of aqueous silica is plotted as a function of temperature and compared to the solubility of quartz and silica glass in Fig. 6.

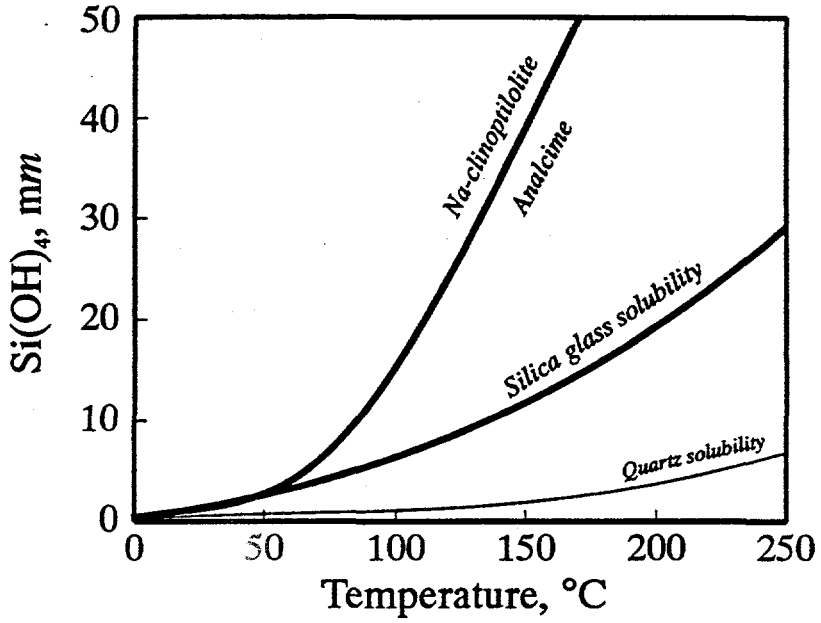

Fig. 6. Plot showing the temperature-dependent silica concentration (assumes silica activity and concentration are equivalent) marking the boundary between analcime and Na-clinoptilolite stability fields (see eqn. 11) in comparison to the solubility of silica glass and quartz.

Based on a metastable equilibrium model, if the solubility of silica glass is taken as the maximum allowed silica concentration in solution, the data in Fig. 6 indicate that Na-clinoptilolite would never persist above ~50°C. The fact that clinoptilolite does persist to temperatures ~150°C (Kristmannsdottir and Tomasson, 1978; Bish and Aronson, 1993) indicates that the Na-clinoptilolite-analcime reaction is a kinetically controlled process. The deviation between the two bold lines in Fig. 6 is a measure of the reaction affinity of the replacement reaction (equation 10). The reaction affinity rapidly increases at temperatures above ~125-150°C; thus, it is expected that the rate of conversion would also rapidly increase in this temperature interval. The apparent control of aqueous silica concentration on the conversion, i.e., dropping from amorphous silica- to quartz-saturated concentrations, may in fact be related to an increase in reaction affinity rather than to an equilibrium control on the reaction. Note that the replacement of Na-clinoptilolite by analcime with a high Si/Al ratio will shift the upper curve on Fig. 6 to slightly higher silica activites at any given temperature; thus, increasing the overall affinity of reaction 10 relative to replacement by a low Si/Al analcime..

CONCLUSIONS

Solubility measurements of zeolites made in aqueous solutions are a useful and comparatively direct method to evaluate thermodynamic properties of zeolite minerals while ensuring that a constant state of hydration is maintained. Precise control of clinoptilolite compositions can be made via cation exchange prior to solubility measurements. In this way solubility products and derived thermodynamic constants can be determined for Na-, K-, Ca-, and Mg-endmember compositions as well as solid

solution compositions. The solubility products determined are necessary for equilibrium and kinetic modeling of zeolite diagenesis and for the design of kinetic experiments where zeolite dissolution and precipitation rates are measured as a function of reaction affinity.

KINETICS OF NA-CLINOPTILOLITE DISSOLUTION & PRECIPITATION AT 125°C

Introduction

Below are described the experimental methods to measure the rates of clinoptilolite dissolution and precipitation in hydrothermal solutions (to ~300°C and ~20MPa). Results of dissolution and precipitation experiments at 125°C are also listed in Table 3. These data are presented and fully discussed along with dissolution data at 25°, 50°, and 80°C in a manuscript prepared by our colleagues at Yale University.

Methods

Rates of Na-clinoptilolite dissolution and precipitation at temperatures above 100°C were measured using a dual-input flow-through reactor system (Soong, 1993). The design of the reactor system allows for the strict control of temperature, pressure, flow rate, and inlet solution saturation states with respect to Na-clinoptilolite, so that dissolution and precipitation rates can be measured as function of ΔG_R. Input solutions were prepared from N_2-purged, doubly distilled, and deionized water. The N_2-gas purging minimizes the amount of dissolved oxygen (see Butler et al., 1994) that rapidly corrodes stainless steel surfaces at elevated temperatures. The pH of the input solution

was buffered to between 8.1 and 8.4 at 25°C with a 5 m*m* $Na_2B_4O_7 \cdot 10H_2O$-7 m*m* HCl solution.

Input solutions were stored in a sealed polyethylene container and pumped by two high-pressure liquid chromatography pumps allowing for flow rates from 0.02 to 20 mL/min (SSI Acuflow). The solution enters two Ti 17 alloy nutrient vessels (1100 mL nominal volume) containing amorphous silica glass and boehmite, respectively. These nutrient vessels are housed in stationary, dual-wound furnaces; thus, the concentrations of dissolved Si and Al leaving the nutrient vessels can be separately controlled via the temperature-dependent solubilities of silica glass and boehmite, respectively. The solutions then pass through heated capillary tubing and mix in a tee-assembly prior to entering a 29 cm^3 Ti 17 alloy reaction vessel contained within a furnace. Mineral samples are placed within the reaction vessel on a 1 μm stainless steel filter separated from a cone-shaped mixing chamber located on the inlet side of the reaction vessel. The temperature in the reaction vessel was measured to ±1.5°C using two chromel-alumel thermocouples (Thermoelectrics Company) inserted into the top and bottom of the vessel. Temperature gradients of less than 2°C were maintained in the reaction vessel. The pressure of the entire system was maintained at *ca.* 17MPa by a back pressure regulator, a condition above the liquid-vapor pressure of the high-temperature solutions ensuring that only a liquid phase was present in the system. Solutions leaving the reactor vessel were collected at the downstream end of the back pressure regulator. A series of valves allows for solutions both leaving and entering the reaction vessel to be sampled.

At the beginning of an experiment, a known mass of Na-clinoptilolite was placed in the reaction vessel, the temperature of the reaction vessel and nutrient vessels were

increased to the desired values, and after a period of several days solution was pumped through the system. Output solutions were collected, filtered through 0.2 μm syringe filters (Nalgene), acidified with Ultrex HNO_3, and analyzed for Na, Al, and Si using inductively-coupled plasma emission spectroscopy (ICP; Leeman Labs PS3000). Accuracy and precision of these analyses were determined from repeated analyses of NIST-traceable standard solutions and are both within ±3% at the 1σ confidence level. pH measurements were made with a semi-micro combination electrode (Corning) calibrated with NIST-traceable buffer solutions and a Corning model 250 ion analyzer. The difference between input and output pH values was generally <0.10 pH units. Rate calculations are made based on the difference between input and output Si concentrations at steady state following equation (#; see Yale report). Steady state output concentrations were generally attained in less than 100 hours of reaction time at 125°C. After several rate measurements the reaction vessel was opened and the contents characterized using powder X-ray diffraction techniques and scanning electron microscopy. These studies did not reveal the presence of any secondary phase formed during the dissolution/precipitation experiments.

Note that although we see a systematic trend of dissolution rates at progressively more unsaturated conditions, the calculated errors are very large close to equilibrium. This is because, to measure rates near equilibrium at 125°C, input solutions must be concentrated in Si. It is difficult to get a large amount of Al into solution because boehmite is relatively insoluble. Using concentrated Na solutions is deleterious to the HPLC pumps over extended runs. Thus we are left with Si to support the ΔG of the input solutions, which note, is cut in 1/2 of what leaves the Si feeder bomb, i.e., if one

Table 3. Na-clinoptilolite dissolution and rate data at 125°C.

Exp.	T (°C)	pH 25	Flow Rate (mL/min)	Mass (g)	Area (m^2)	Time (hours)	Rate Si mol/m^2s	Error	Affinity (kcal/mol)
A1	125	8.18	4.16	0.074	1.443	20	2.3e-10	±2.4e-10	4.01
A2	125	8.23	4.16		1.443	23	1.4e-10	±2.5e-10	2.00
A3	125	8.11	4.16		1.443	49	-2.0e-10	±2.1e-10	-3.10
A4	125	8.11	4.16		1.443	69	-2.5e-10	±1.5e-10	-8.10
A5	125	8.15	4.16		1.443	31	-2.5e-10	±1.5e-10	-10.20
A6	125	8.09	4.16		1.443	45	-4.5e-10	±0.8e-10	-14.93
A7	125	8.06	4.16		1.443	29	-4.4e-10	±0.8e-10	-15.66
A8	125	8.07	4.16		1.443	31	-2.9e-10	±1.4e-10	-8.19
B1	125	8.25	4.50	0.096	1.872	67	-1.6e-10	±1.6e-10	-8.38
B2	125	8.28	4.50		1.872	81	-5.1e-10	±0.5e-10	-23.67
C1	125	8.41	3.90	0.103	2.000	70	-1.2e-10	±2.0e-10	-7.10
C2	125	8.36	3.90		2.000	67	-4.2e-10	±0.8e-10	-26.95
C3	125	8.41	3.90		2.000	45	-7.3e-10	±0.5e-10	-34.60

requires concentration x of silica entering the reaction vessel, concentration 2x must leave the Si nutrient bomb. The rate measurement is based on the difference between input and output silica concentration which is small close to equilibrium; consequently, the error is assessed because we are looking at a small difference between two relatively large values. To mobilize large amounts of silica in solution, we have gone to using silica glass rather than quartz but this method is not without problems as we have occasionally had silica precipitate out in the lines leading to the reaction vessel.

FUTURE ACTIVITIES

The methods and materials developed in this study for the measurement of zeolite solubilities and rates of dissolution and precipitation make possible a large number of

possible experiments of interest to the YMP project. Some of these possibilities are summarized below:

(1) Although dissolution and precipitation rate data have been obtained for Na-clinoptilolite at 125°C, these measurements need to be extended to 175°C. Experiments at 175°C are nearly underway. The dissolution kinetics may represent a rate-controlling step of the clinoptilolite-analcime reaction and at least provide constraints on the rate of the conversion reaction. We have planned experiments to test the possibility of experimentally tracking the clinoptilolite-analcime reaction.

(2) The determination of analcime dissolution and precipitation kinetics should be comparatively easy compared to measuring clinoptilolite rates because of the much lower solubility of analcime. Relatively little preparation is now required to measure analcime reaction rates as a function of, for example, T and reaction affinity.

(3) By cation-exchanging Castle Creek clinoptilolite, end-member compositions can be prepared and used in solubility measurements. We currently are working on measuring the solubility of K- and Ca-clinoptilolite. This work should be extended to Mg compositions and solid solution compositions which may potentially lead to a relatively complete assessment of clinoptilolite thermodynamic properties.

(4) There is currently a dearth of information available on mordenite thermodynamical properties. Such information is certainly of interest to the YMP. We presently have a

small supply of Na-exchanged mordenite that could be used in both solubility and kinetic experiments.

REFERENCES CITED

Barnes, H.L. (1971) Investigations in hydrothermal sulfide systems. In *Research Techniques for High Pressure and High Temperature* (ed. G.C. Ulmer). Springer-Verlag.

Bish, D.L. (1984) Effects of exchangeable cation composition on the thermal expansion/contraction of clinoptilolite. *Clays and Clay Minerals*, v. 32: 444-452.

Bish, D.L. and Aronson, J.L. (1993) Paleogeothermal and paleohydrologic conditions in silicic tuff from Yucca Mountain, Nevada. *Clays and Clay Minerals*, v. 41: 148-161.

Boles, J.R. (1971) Synthesis of analcime from natural heulandite and clinoptilolite. *American Mineralogist*, v. 56: 1724-1734.

Boles, J.R. (1972) Composition, optical properties, cell dimensions, and thermal stability of some heulandite group zeolites. *American Mineralogist*, v. 57: 1463-1493.

Boles, J.R. (1985) Occurrences of natural zeolites - present status and future research. In *Occurrence, Properties, and Utilization of Natural Zeolites* (eds. D. Kallo and H.S. Sherry), pp. 3-18, Akademiai Kiado.

Bourcier, W.L. and Barnes, H.L. (1987) Rocking autoclaves for hydrothermal experiments I. Fixed volume systems. In *Hydrothermal Experimental Techniques* (eds. G.C. Ulmer and H.L. Barnes). John Wiley & Sons.

Bourcier, W.L., Knauss, K.G., and Jackson, K.J. (1993) Aluminum hydrolysis constants to 250°C from boehmite solubility experiments. *Geochimica et Cosmochimica Acta*, v. 57: 747-752.

Bowers, T.S. and Burns, R.G. (1990) Activity diagrams for clinoptilolite: Susceptibility of this zeolite to further diagenetic reactions. *American Mineralogist*, v. 75: 601-619.

Butler, I.B., Schoonen, M.A.A., and Rickard, D.T. (1994) Removal of dissolved oxygen from water: A comparison of four common techniques. *Talanta*, v. 41: 211-215.

Castet, S., Dandurand, J., Schott, J., and Gout, R. (1993) Boehmite solubility and aqueous aluminum speciation in hydrothermal solutions (90°-350°C):

Experimental study and modeling. *Geochimica et Cosmochimica Acta*, v. 57: 4869-4884.

Chen, C.A. and Marshall, W.M. (1982) Amorphous silica solubility IV. Behavior in pure water and aqueous sodium chloride, sodium sulfate, magnesium chloride, and magnesium sulfate solutions up to 350°C. *Geochimica et Cosmochimica Acta*, v. 46: 279-287.

Cobble, J.W., Murray, R.C., Turner, P.J., and Chen, K. (1982) *High-Temperature Thermodynamic Data for Species in Aqueous Solution.* Electric Power Research Institute

Gammons, C.H. and Barnes, H.L. (1989) The solubility of Ag_2S in near-neutral aqueous sulfide solutions at 25 to 300°C. *Geochimica et Cosmochimica Acta*, v. 53: 279-290.

Gingele, F.X. and Schulz, H.D. (1993) Authigenic zeolites in Late Pleistocene sediments of the South Atlantic (Angola Basin). *Marine Geology*, v. 111: 121-131.

Hay, R.L. (1978) Geologic occurrence of zeolites. In *Natural Zeolites: Occurrence, Properties, Use* (eds. L.B. Sand and F.A. Mumpton), pp. 135-143. Pergamon

Helgeson, H.C. (1969) Thermodynamics of hydrothermal systems at elevated temperatures and pressures. *American Journal of Science*, v. 63: 622-635.

Hemingway, B.S. and Robie, R.A. (1984) Thermodynamic properties of zeolites: Low temperature heat capacities and thermodynamic functions of phillipsite and clinoptilolite. Estimates of the thermochemical properties of zeolitic water at low temperatures. *American Mineralogist*, v. 69: 692-700.

Howell, D.A., Johnson, G.K., Tasker, I.R., O'Hare, P.A.G., and Wise, W.S. (1990) Thermodynamic properties of the zeolite stilbite. *Zeolites*, v. 10: 525-531.

Iijima, A. and Utada, M. (1966) Zeolites in sedimentary rocks, with reference to the depositional environments and zonal distribution. *Sedimentology*, 7: 327-357.

Johnson, G.K., Flotow, H.E., and O'Hare, P.A.G. (1983) Thermodynamic studies of zeolites: natrolite, mesolite, and scolecite. *American Mineralogist*, v. 68: 1134-1145.

Johnson, G.K., Flotow, H.E., O'Hare, P.A.G., and Wise, W.S. (1982) Thermodynamic studies of zeolites: analcime and dehydrated analcime. *American Mineralogist*, v. 67: 736-748.

Johnson, G.K., Flotow, H.E., and O'Hare, P.A.G. (1985) Thermodynamic studies of zeolites: heulandite. *American Mineralogist*, v. 70: 1065-1071.

Johnson, G.K., Tasker, I.R., Flotow, H.E., O'Hare, P.A.G., and Wise, W.G. (1992) Thermodynamic studies of mordenite, dehydrated mordenite, and gibbsite. *American Mineralogist*, v. 77: 85-93.

Kastner, M. And Stonecipher, S.A. (1978) Zeolites in pelagic sediments of the Atlantic, Pacific, and Indian Oceans. In *Natural Zeolites: Occurrence, Properties, Use* (eds. L.B. Sand and F.A. Mumpton), pp. 199-220. Pergamon

Kerrisk, J.F. (1983) Reaction-path calculations of groundwater chemistry and mineral formation at Rainier Mesa, Nevada. *U.S. National Technical Information Service, Report LA-10929.*

Kharaka, Y.K., Gunter, W.D., Aggarwal, P.K., Perkins, E.H., and DeBraal, J.P. (1988) SOLMINEQ88: A computer program for geochemical modeling of water-rock interactions. *U.S. Geological Survey, Water Investigations Report 88-4227.*

Kristmanndottir, H. And Tomasson, J. (1978) Zeolite zones in geothermal areas of Iceland. In *Natural Zeolites: Occurrence, Properties, Use* (eds. L.B. Sand and F.A. Mumpton), pp. 277-284. Pergamon.

Mondale, K.D., Mumpton, F.A., and Aplan, F.F. (1988) Properties and beneficiation of natural sedimentary zeolites. In *Process Mineralogy VIII* (eds. D.J.T. Carson and A.H. Vassiliou).

Mumpton, F.A. (1978) Natural zeolites: a new industrial mineral commodity. In *Natural Zeolites: Occurrence, Properties, Use* (eds. L.B. Sand and F.A. Mumpton), pp. 3-27. Pergamon.

Pabalan, R.T. (1994) Thermodynamics of ion exchange between clinoptilolite and aqueous solutions of Na^+/K^+ and Na^+/Ca^{2+}. *Geochimica et Cosmochimica Acta*, v. 58: 4573-4590.

Rimstidt, J.D. and Barnes, H.L. (1980) The kinetics of silica-water reactions. *Geochimica et Cosmochimica Acta*, v. 44: 1683-1699.

Sheppard, R.A. and Gude, A.J. III (1969) Diagenesis of tuffs in the Barstow Formation, Mud Hills, San Bernardino County, California. *U.S. Geological Survey Professional Paper 597*, pp. 1-38.

Soong, C. (1993) Hydrothermal kinetics of kaolinite-water interaction at pH 4.2 and 7.3, 130° to 230°C. Ph.D. dissertation, The Pennsylvania State University.

Surdam, R.C. and Sheppard, R.A. (1978) Zeolites in saline, alkaline-lake deposits. In *Natural Zeolites: Occurrence, Properties, Use* (eds. L.B. Sand and F.A. Mumpton), pp. 145-174. Pergamon

Wesolowski, D.J. and Palmer, D.A. (1994) Aluminum speciation and equilibria in aqueous solution: V. Gibbsite solubility at 50°C and pH 3-9 in 0.1 molal NaCl solutions (a general model for aluminum speciation; analytical methods). *Geochimica et Cosmochimica Acta*, v. 58: 2947-2969.

Wise, W.S. (1984) Thermodynamic studies of zeolites: Analcime solid solutions. In *Proceedings of the Sixth International Zeolite Conference* (eds. D. Olson and A. Bisio), pp. 616-623. Butterworths.

Wilkin, R.T. and Barnes, H.L. (1995) Solubilities of the zeolites analcime and Na-clinoptilolite in hydrothermal solutions. *V.M. Goldschmidt Conference Program and Abstracts, p. 97.*

APPENDIX A

X-ray powder diffraction patterns of A) Castle Creek Na-clinoptilolite; and B) Mont St. Hilaire analcime. The patterns were obtained using Cu Kα radiation and a scan step of 0.05° 2-theta

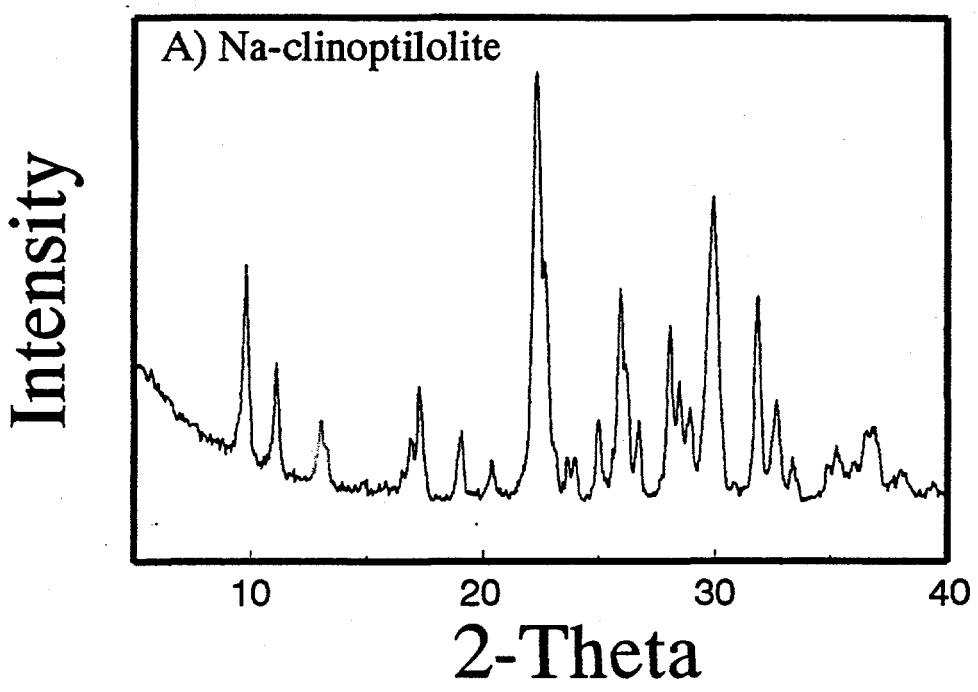

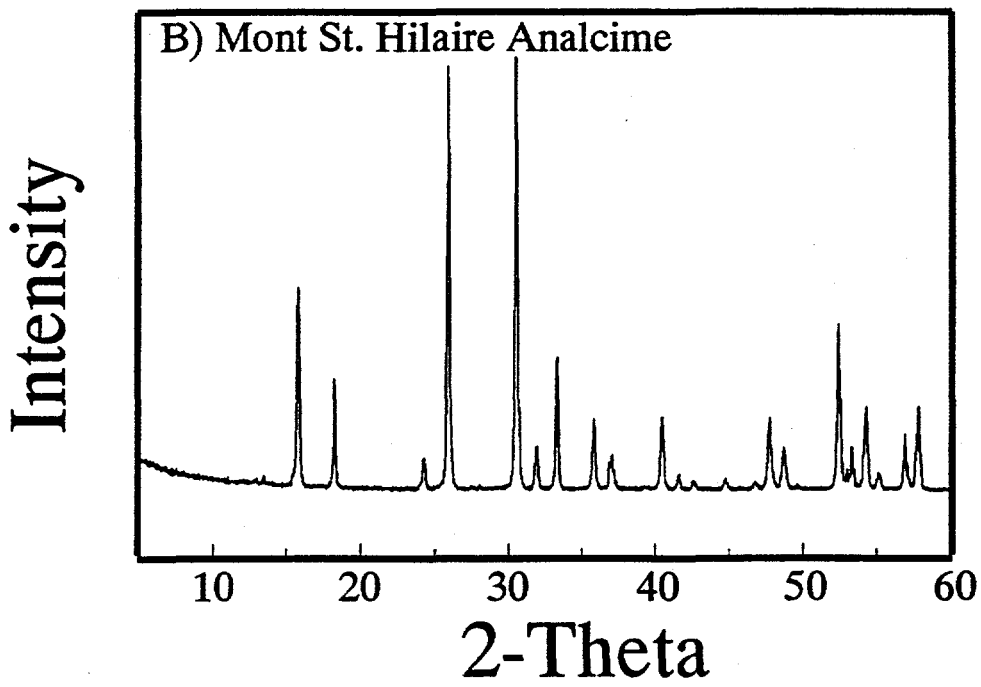

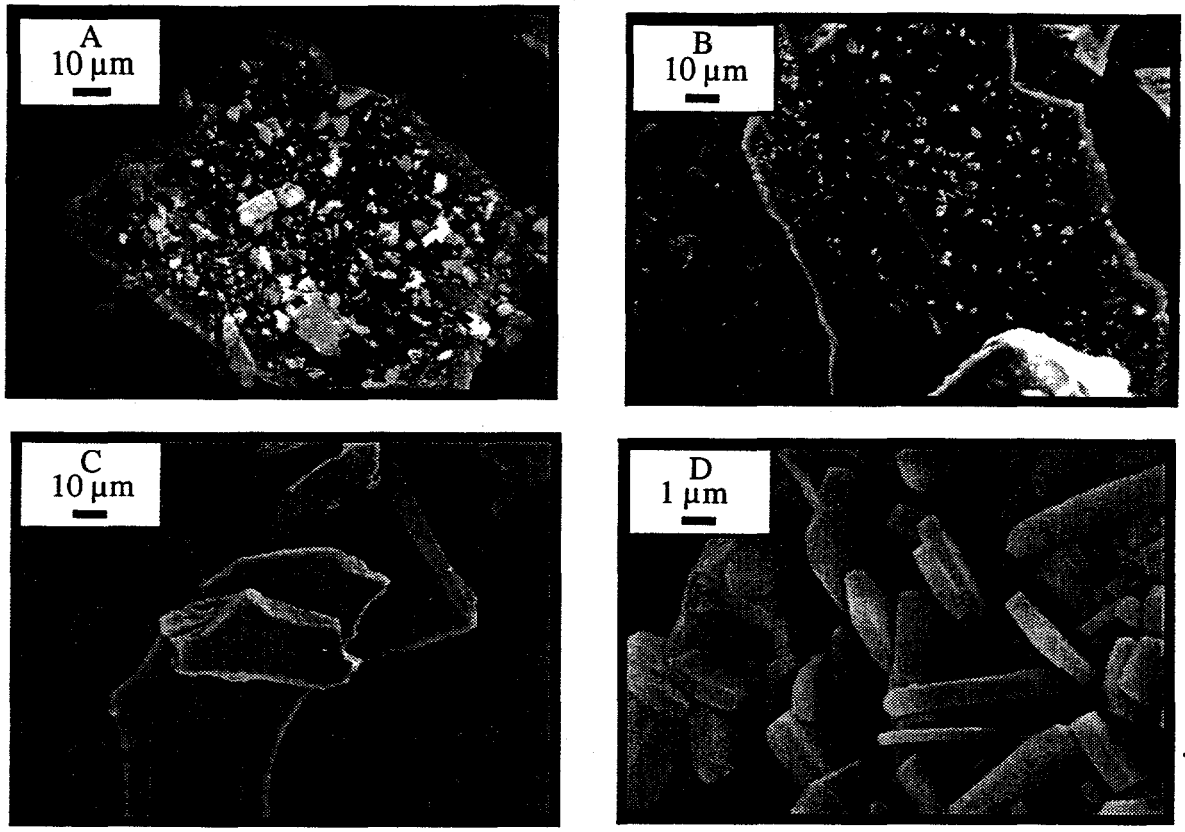

APPENDIX A (cont.)

SEM photomicrographs of zeolites. (A) Mont St. Hilaire analcime after crushing and seiving. (B) Mont St. Hilaire analcime after ultra-sonic cleaning treatment. (C) Mont St. Hilaire after hydrothermal treatment (120°C for 2 weeks). Note analcime grains are free of ultra-fine particles. (D) Hydrothermally treated Na-clinoptilolite.

APPENDIX B

Experimental solubility data

Sample	Temperature	Time (hours)	ΣSi (m*m*)	ΣAl (m*m*)	ΣNa (m*m*)	pH_{25}	Direction	log K_{sp}
Mont St. Hilaire analcime								
21	90	787	1.20	0.14	0.22	8.28	↑	-13.33
22	90	787	1.11	0.14	0.30	8.28	↑	-13.27
27	125	576	0.88	0.39	2.55	8.70	↑	-12.13
28	125	576	0.85	0.38	2.50	8.70	↑	-12.18
29	125	576	0.84	0.37	2.45	8.70	↑	-12.22
30	175	24	1.52	0.79	2.17	na	↑	-11.42
31	175	48	1.64	0.87	2.14	na	↑	-11.32
32	175	98	1.56	0.82	2.10	na	↑	-11.40
33	175	170	1.46	0.73	1.89	na	↑	-11.55
34	175	482	1.54	0.73	2.23	9.47	↑	-11.45
35	175	482	1.51	0.73	2.25	9.47	↑	-11.46
36	225	119	2.56	1.45	3.16	9.82	↑	-10.59
37	225	119	2.52	1.49	3.16	9.82	↑	-10.59
38	275	98	3.68	1.59	3.29	9.16	↑	-10.23
39	275	98	3.63	1.61	3.31	9.16	↑	-10.24
46	300	35	4.31	1.61	2.39	8.42	↑	-10.24
47	300	35	4.37	1.62	2.49	8.42	↑	-10.21
48	275	47	4.42	1.34	2.24	8.85	↓	-10.31
49	275	47	4.49	1.36	2.27	8.85	↓	-10.29
50	275	47	4.35	1.28	2.21	8.85	↓	-10.35
51	225	52	3.76	0.89	2.17	8.65	↓	-10.63
52	225	52	3.72	0.87	2.07	8.65	↓	-10.67
60	175	24	2.73	0.34	1.96	na	↓	-11.34
61	175	50	2.51	0.29	1.83	na	↓	-11.50
62	175	73	2.50	0.28	1.86	na	↓	-11.51
64	175	119	2.42	0.27	1.86	na	↓	-11.56
67	175	193	2.32	0.27	1.88	8.15	↓	-11.60
68	175	193	2.41	0.30	1.92	8.15	↓	-11.50
71	125	22	2.11	0.20	1.76	na	↓	-11.83
72	125	44	1.95	0.20	1.82	na	↓	-11.86
73	125	92	1.76	0.15	1.77	na	↓	-12.11
76	125	198	1.66	0.11	1.76	7.97	↓	-12.28
77	125	198	1.70	0.11	1.79	7.97	↓	-12.25
78	90	89	1.55	0.07	1.83	7.64	↓	-12.53
83	90	326	1.40	0.04	1.72	7.37	↓	-12.92
84	90	374	1.37	0.04	1.69	7.35	↓	-12.94
86	90	432	1.36	0.04	1.73	7.33	↓	-12.95
Wikieup analcime								
108	125	196	3.24	0.12	1.32	9.15	↑	-11.30
109	125	196	3.28	0.12	1.30	9.15	↑	-11.29
114	175	93	7.61	0.19	1.39	8.82	↑	-10.25
115	175	93	7.68	0.19	1.36	8.82	↑	-10.25
116	225	48	14.56	0.33	2.06	8.95	↑	-9.35
117	225	48	14.66	0.33	2.05	8.95	↑	-9.35
123	175	49	13.65	0.16	2.38	8.87	↓	-9.62
124	175	49	13.71	0.16	2.39	8.87	↓	-9.59
127	125	117	10.56	0.02	1.86	8.88	↓	-10.71

128	125	117	10.77	0.03	1.85	8.88	↓	-10.65
131	90	483	4.78	0.005	1.43	8.80	↓	-12.04
132	90	483	4.55	0.005	1.36	8.80	↓	-12.05
Castle Creek Na-clinoptilolite								
1	125	339	4.20	0.11	3.04	6.84	↑	-18.86
2	125	339	3.74	0.06	2.59	6.84	↑	-19.44
3	125	339	4.44	0.11	2.44	6.84	↑	-18.86
4	175	170	7.24	0.41	3.65	8.31	↑	-16.82
5	225	103	12.51	0.54	4.02	8.63	↑	-15.50
7	265	77	18.67	0.51	4.27	8.80	↑	-14.56
8	265	77	16.24	0.58	4.20	8.80	↑	-14.93
9	200	96	11.43	2.02	0.29	8.76	↓	-16.29
10	200	96	9.49	0.32	1.93	8.76	↓	-16.66
11	175	122	8.46	0.38	1.33	8.74	↓	-16.99
12	175	122	10.19	0.21	1.43	8.74	↓	-16.82
13	125	280	7.62	0.07	1.14	8.81	↓	-18.10
14	125	280	6.69	0.18	1.11	8.81	↓	-17.91
16	225	245	15.72	0.36	1.61	8.44	↑	-15.64
17	225	245	16.20	0.74	1.85	8.44	↑	-15.17
23	90	1080	3.62	0.02	0.23	7.36	↑	-21.02
24	90	1080	3.60	0.02	0.33	7.36	↑	-20.90
55	100	360	3.34	0.09	0.65	8.21	↑	-19.90
56	100	360	3.45	0.05	0.59	8.21	↑	-20.16
74	100	697	3.98	0.19	0.84	8.91	↑	-19.08
75	100	697	3.49	0.19	0.72	8.91	↑	-19.43
79	125	122	5.21	0.30	1.18	8.24	↑	-18.14
80	125	338	5.20	0.35	1.26	8.49	↑	-18.03
81	125	338	5.08	0.31	1.22	8.49	↑	-18.15
85	125	407	5.00	0.33	1.22	8.51	↑	-18.16
87	125	465	4.81	0.29	1.23	8.53	↑	-18.30
89	125	625	4.91	0.29	1.44	8.51	↑	-18.19
91	100	48	4.36	0.17	1.17	8.47	↓	-18.79
92	100	216	4.04	0.13	1.11	8.49	↓	-19.09
95	100	885	3.61	0.15	1.09	8.53	↓	-19.29

Notes: pH measurement was at 25°C; (↑) indicates measurements made from undersaturated conditions; (↓) indicates measurements from supersaturated conditions. na stands for not available.

APPENDIX C

Free energies of formation of aqueous species and zeolites determined in this study

Temperature (°C)	$\Delta G°_f$ (kJ/mol) Na^+	$Al(OH)_4^-$	$Si(OH)_4$	$H_2O(l)$	Mont St. Hilaire Analcime	Wikieup Analcime	Castle Creek Na-clinop.
25	-261.9	-1305.4	-1308.1	-237.2	-3105.3		-6262.9
50	-263.8	-1289.2	-1295.7	-233.2	-3080.5		-6213.8
80	-266.2	-1269.7	-1281.0	-228.4	-3048.1		-6159.7
90	-266.9	-1262.8	-1276.1	-226.8	-3036.2	-2989.0	-6130.9
100	-267.7	-1255.9	-1271.2	-225.2	---	---	-6105.5
125	-269.6	-1239.1	-1259.0	-221.3	-3010.4	-2961.7	-6062.6
175	-273.3	-1207.3	-1234.8	-213.7	-2977.5	-2925.2	-5985.0
200	-275.2	-1191.0	-1222.8	-210.0	---	---	-5946.5
225	-276.9	-1174.3	-1210.8	-206.3	-2939.8	-2889.8	-5900.8
265	-279.2	-1147.8	-1191.6	-200.4	---	---	-5835.5
275	-279.7	-1141.6	-1186.8	-199.0	-2905.0	---	---
300	-280.2	-1124.7	-1174.9	-195.4	-2887.2	---	---